Two-Step Folding of Recombinant Mitochondrial Porin in Detergent

Denice C. Bay,* Joe D. O'Neil,† and Deborah A. Court*
Departments of *Microbiology and †Chemistry, University of Manitoba, Winnipeg, Manitoba R3T 2N2, Canada

ABSTRACT Precise information regarding the transmembrane topology of mitochondrial porin is essential for understanding the mechanisms by which this protein functions. Porin acts as a channel in the outer membrane and interacts with small solutes and proteins to regulate mitochondrial function. The acquisition of high-resolution structural data requires a method of maintaining high concentrations of unaggregated, properly folded porin. In the current studies, several mixed detergent systems were analyzed for their ability to fold *Neurospora* mitochondrial porin expressed in and isolated from *Escherichia coli*. A mixture of sodium dodecyl sulfate and dodecyl-β-D-maltopyranoside in a 1:6 molar ratio supports a β-strand-rich conformation. In this state, the two tryptophan residues in the protein reside in hydrophobic environments, and about half of the nine tyrosines are solvent exposed. Most importantly, heat-labile tertiary contacts, as detected by near-UV circular dichroism spectropolarimetry, in the sodium dodecyl sulfate/dodecyl-β-D-maltopyranoside-solubilized porin are very similar to those of the protein following functional reconstitution into liposomes. Similarly, both forms are protease resistant. Thus, a method has been identified with the potential to solubilize high concentrations of mitochondrial porin in a state virtually indistinguishable from the membrane-embedded form.

INTRODUCTION

One of the most abundant proteins in the mitochondrial outer membrane is mitochondrial porin, otherwise known as VDAC. Like its bacterial namesakes, this channel is presumed to exist in a β-barrel composed of antiparallel transmembrane β-strands (see Fig. 1 for one model). Reconstitution of these proteins into artificial membranes generates channels that passively transport solutes and display voltage-dependent gating; the channels are ''open'' and anion selective at low applied voltages and exist in partially closed, cation-selective states on application of high voltages (reviewed by Benz (1)).

Mitochondrial porins have been shown to interact with small molecules and other proteins that participate in a variety of cellular processes. Examples of interaction partners include hexokinase (2) and creatine kinase (3), which are involved in glucose metabolism. ATP (4,5), NADH (6), and the inner membrane ATP/ADP carrier (reviewed by Crompton et al. (7)) also interact with porin and participate in processes involving oxidative phosphorylation. Furthermore, regulators of apoptosis, namely the Bcl-2 family of proteins (as reviewed elsewhere (8,9)) interact with VDAC in higher organisms, potentially controlling cytochrome *c* release and the induction of apoptosis. In many cases, these interactions modulate channel gating and reflect complex interactions of porin with its environment (reviewed by Blachly-Dyson and Forte (10)). The involvement of mitochondrial porin in multiple cellular activities emphasizes the need for understanding the structural arrangement of this channel. However, in contrast to the wealth of information regarding bacterial porin structure, very little is known about the topology of mitochondrial porins.

Evidence supporting a β-barrel conformation for mitochondrial porins has included structural predictions based on primary sequence, the properties of porin channels in artificial membranes, and far-UV CD spectropolarimetry studies (40–70% β-strand) (11–14). Low-resolution electron microscopic analysis of two-dimensional and multilamellar arrays confirmed the barrel structure of porin (15–18). Other direct approaches to the determination of mitochondrial porin structure have been hindered by the low yields of folded protein obtained from mitochondria, the low solubility of the recombinant protein in the detergents used for electrophysiological analysis, and the poor stability of mitochondrial porins in comparison to their bacterial counterparts (19,20).

Isolation of native mitochondrial porin in quantities high enough for spectroscopic analysis (microgram amounts) requires a large quantity of cells and numerous purification steps involving initial solubilization in detergent (21–25). The low yields of protein restrict the techniques available for the characterization of the folded state. Recombinant His_6-porin expressed in *Escherichia coli* has facilitated the purification of higher quantities of protein (milligrams), but at the cost of the native folded state, because these proteins must be isolated from inclusion bodies (9,13,26). Isolation

Submitted June 14, 2007, and accepted for publication September 4, 2007.

Address reprint requests to Deborah A. Court, Dept. of Microbiology, University of Manitoba, Winnipeg, MB R3T 2N2, Canada. Tel.: 204-474-8263; Fax: 204-474-7603; E-mail: Deborah_Court@umanitoba.ca.

Abbreviations used: VDAC, voltage-dependent anion-selective channel; BOC, *N-t*-butyloxycarbonyl; CMC, critical micelle concentration; UV, ultraviolet; CD, circular dichroism; DDM, dodecyl-β-D-maltoside; DPC, dodecyl phosphocholine; FT, freeze-thaw; HT, high tension; hVDAC1, isoform 1 of human voltage-dependent anion channel; LDAO, lauryl dimethylamine oxide; λ_{max}Trp, wavelength at which tryptophan-derived fluorescence emission is at maximum value; λ_{min}, wavelength minimum of far-UV spectrum; OG, *n*-octyl-β-D-glucopyranoside; SDS, sodium dodecyl sulfate; SUV, small unilameller vesicles; N-Ac-W-NH_2, *N*-acetyl-tryptophan amide; N-Ac-Y-NH_2, *N*-acetyl-tyrosine amide; N-Ac-W-OEth, *N*-acetyl-tryptophan ethyl ester; BOC-Y-OMe, *N-tert*-butoxycarbonyl-tyrosine methyl ester; PEG, polyethylene glycol.

Editor: Lukas K. Tamm.

0006-3495/08/01/457/12 $2.00

doi: 10.1529/biophysj.107.115196

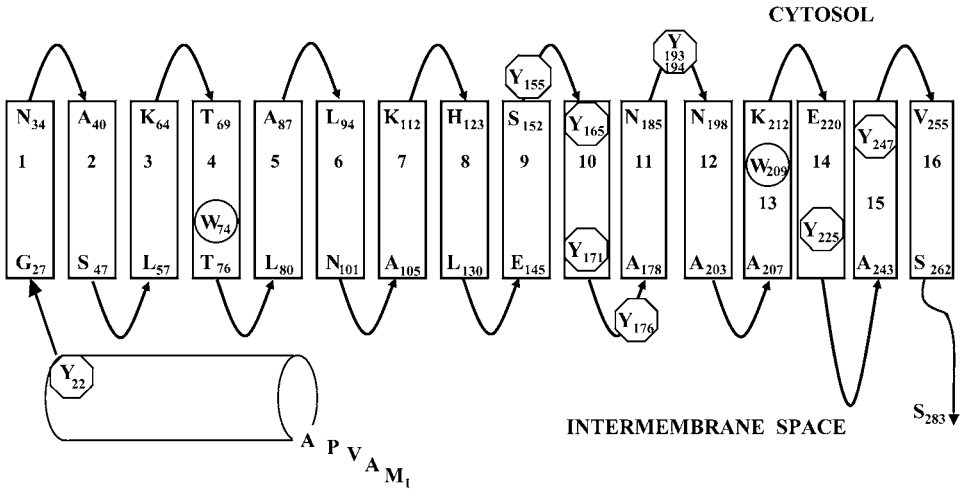

FIGURE 1 Model for the transmembrane arrangement of *Neurospora* mitochondrial porin (20,58). The N-terminus is at the left and proposed to reside in the intermembrane space. Potential β-strands are indicated by rectangles, and loops and turns by arrows between them. The estimated positions of Tyr (Y) and Trp (W) residues are indicated. The putative limits of the β-strands are indicated; it should be noted that neither the number of strands nor the precise position of any one strand has been confirmed by high-resolution methods.

and folding usually have involved denaturation and subsequent solubilization in detergent, using dialysis (13) or dropwise dilution (9) to remove the denaturant while encouraging folding that presumably reflects that of the native porin.

Our recent studies utilizing His-tagged *Neurospora crassa* mitochondrial porin involved spectroscopic characterization of the protein and model compounds in single detergents (26). His_6-porin was purified in 8 M urea, acetone precipitated, and the dried pellet dissolved directly in the detergent of choice. High concentrations of His_6-porin were attainable in LDAO, DPC, and SDS, but high β-strand content was exhibited by the protein in LDAO only.

Alternative detergent systems for solubilizing other membrane proteins involve mixtures of anionic and nondenaturing, nonionic detergents. For example, the *E. coli* integral OmpA has been folded in a mixture of SDS and OG (27–29). SDS and DDM systems have been used for solubilization of other membrane proteins including DsbB (30) and the P5 outer membrane protein of *Haemophilus influenzae* (31). The focus of many of these studies was to characterize unfolding kinetics on the addition of SDS to protein folded in a nonionic detergent (28,32). However, in the case of OmpA, folding into a β-rich conformation could be achieved by adding OG to SDS-solubilized protein at a particular molar ratio of the two detergents (29).

In this study, mixed detergent systems were used to solubilize recombinant His_6-tagged *N. crassa* mitochondrial porin. SDS and DPC were chosen for primary solubilization of the protein based on the high solubility of His_6-porin in these detergents (26). Several nonionic and zwitterionic detergents were added as the secondary surfactants, and varying molar ratios of the two detergents were examined. The folded states of the proteins in the resulting detergent mixtures were examined by CD spectropolarimetry in the far-UV and near-UV regions, by fluorescence spectrophotometry, and by UV absorption spectroscopy. To interpret the results obtained for His_6-porin in these binary systems, aromatic amino acid derivatives of varying hydrophobicity were also examined to probe the micellar environments experienced by the protein. His_6-porin also was reconstituted into liposomes and analyzed by fluorescence and CD spectropolarimetry to provide reference data for the folded porin. Based on these criteria, SDS/DDM-solubilized His_6-porin exhibits a conformation that is virtually indistinguishable from that of the membrane-embedded protein.

MATERIALS AND METHODS

Detergents and amino acid derivatives

DPC, DDM, and OG were purchased from Anatrace (Maumee, OH), and LDAO from Calbiochem (San Diego, CA). Sigma (St. Louis, MO) was the supplier of N-Ac-W-NH_2, N-Ac-Y-NH_2, SDS, urea, and N-Ac-W-OEth). BOC-Y-OMe, egg yolk L-α-phosphatidyl choline, and egg lecithin L-α-phosphatidic acid were purchased from Fluka (Oakville, Ontario,Canada).

Expression and purification of His_6-porin

The construct encoding the N-terminal His_6-tagged version of *N. crassa* has been described previously (33). Recombinant mitochondrial porins that bear N-terminal hexahistidinyl-tags (His_6-porin) are functionally indistinguishable from porins isolated from mitochondrial membranes (33,13).

Protein expression was carried out in QIA*express E. coli* M15 (pREP4) (Qiagen, Toronto, Ontario, Canada). His_6-porin was purified in 8 M urea, as described (26).

Detergent solubilization of His_6-porin

After dialysis against 8 M urea, His_6-porin was acetone-precipitated, and the dried pellets were resuspended either in SDS (3.5 or 21 mM) or DPC (20 or 100 mM), buffered in 50 mM sodium phosphate, pH 7. After mixing by repeated inversion overnight at room temperature (22°–25°C), samples were clarified by centrifugation at 10,000 $\times$ *g* for 15 min. For mixed detergent systems, an appropriate amount of the second detergent, in powder form, was added, and the samples mixed by inversion overnight. Insoluble protein aggregate was removed by centrifugation before analysis.

Liposome stock preparation

SUV were prepared using modifications of procedures described earlier (11). Briefly, a 10:1 (w/w) mixture of egg yolk L-α-phosphatidyl choline and egg lecithin L-α-phosphatidic acid was prepared. Phospholipid was dissolved in chloroform and evaporated in a fume hood at room temperature (22–25°C) overnight. Dried lipids were either stored at −20°C in a desiccator or resuspended in phosphate buffer to a concentration of 40 mg phospholipid/ml for immediate use. The resulting milky suspension was diluted 1:1 with phosphate buffer and sonicated on ice until the microtip (Fisher Scientific (Ottawa, Ontario, Canada) Sonifier Model 300) could be clearly observed to yield the stock SUV suspension.

Proteoliposome preparation and swelling assays

Liposomes were prepared based on a modified procedure for Type B (CD grade) liposomes as described (11). In short, the stock SUV suspension was diluted 1:1 with His_6-porin (0.5 to 1 μM) in 3.5 mM SDS or in $SDS_{3.5}DDM_{30}$. The resulting suspension was subjected to three cycles of freezing in liquid nitrogen for 1 min and thawing for 20 min at room temperature. After the last thawing in the FT cycle, samples were diluted with 1.5 volumes of phosphate buffer, resulting in a cloudy suspension. Negative controls for liposome swelling experiments were prepared with detergents only and lacked His_6-porin.

Assays were also performed to assess the ability of urea- and detergent-solubilized His_6-porin to insert into liposomes (data not shown) as described for *E. coli* OmpA (34). Liposomes for porin insertion experiments were prepared as described above for liposome swelling except that the stock 20 mg/ml SUV suspension was diluted 1:1 with phosphate buffer. After the three FT cycles, 0.25 volumes of detergent-resuspended porin and 1.25 volumes of phosphate buffer were added to create a final 1:1.5 dilution. To encourage insertion, samples were incubated overnight at room temperature, 30°C, and 42°C.

Liposome swelling (11,35) was measured on an Ultrospec 3100 pro spectrophotometer at an absorbance of 400 nm. Liposome samples prepared as described above were diluted 1/100 into sodium phosphate buffer to a final volume of 0.5 ml and measured in a 1-cm quartz cuvette. After 300–400 s, liposomes were shocked with 40 μl of the isosmotic phosphate buffer, pH 7, followed by an addition of 40 μl of 1 M sucrose (11) or 40 μl of 0.5 g/ml (PEG, Sigma, average molecular weights of 1000 or 3350 (35)), after 600–700 s. Liposome reswelling, as indicated by a gradual decrease in $A_{400\ nm}$, was followed for up to 1800 s after sucrose addition.

Protease digestions of mitochondria and His_6-porin in liposomes or mixed detergents

Mitochondria were isolated from *N. crassa 97-20 mus his*$^-$ (36) according to the method described by (37). Mitochondrial pellets were resuspended in SEM (250 mM sucrose, 1 mM EDTA, 9 mM MOPS, pH 7.5), 3.5 mM SDS or $SDS_{3.5}DDM_{30}$ to a final concentration of 1 mg/ml mitochondrial protein as determined by a Bradford assay (Sigma). Mitochondrial digestions contained 0.5 mg/ml mitochondrial protein in 1.75 mM SDS and 15 mM DDM. All samples were digested with a final concentration of 0.15 mg/ml trypsin for 10 or 30 min at room temperature.

His_6-porin in detergent was digested with trypsin under the same conditions as for mitochondria. Final concentrations of samples were as follows: 0.075 mg/ml (2.5 μM) His_6-porin, 1.75 mM SDS, and 15 mM DDM. All protease digestions were stopped by the addition of phenylmethylsulfonlyfluoride to a final concentration of 20 mM and 4:1 dilution into 5× Laemmli buffer (38) containing 8 M urea. As a control for protease activity in the SDS/DDM system, bovine serum albumin (Sigma) was also digested under these conditions and demonstrated susceptibility to trypsin (data not shown).

All protease-digested samples were loaded onto 0.1% SDS, 3 M urea, 14% polyacrylamide gels; the urea was necessary to aid migration of the protein in the presence of high concentrations of lipid. After electrophoresis and Western blotting, the samples were probed with an antibody against residues 7–20 of *N. crassa* mitochondrial porin (α-NcPor-N) generated by R. Lill at Universität München.

Fluorescence spectrophotometry

Fluorescence spectroscopic analyses of detergent-solubilized model compounds and His_6-porin were performed using a Shimadzu RF-1501 fluorometer or a JASCO-810 (FMO-427S) spectropolarimeter/fluorometer, as described (26). The relatively hydrophilic (N-Ac-W-NH_2 and N-Ac-Y-NH_2) and hydrophobic (BOC-Y-OMe and N-Ac-W-OEth) model compounds were used for comparison with fluorescence by His_6-porin. Samples of individual model compounds, and Trp:Tyr mixtures in the same molar ratio as in His_6-porin (2:9), were prepared at molar concentrations close to those of the individual residues in porin, and all of the protein and model compound fluorescence spectra were normalized with reference to His_6-porin in urea.

UV absorption spectroscopy

UV absorption spectra were obtained on an Ultrospec 4000 spectrophotometer, as described (26). Tyrosine exposure (α) was calculated using the method described by Bay (26) and in Ragone et al. (39). UV absorption spectra of proteoliposomes could not be reliably measured because of high light scatter.

CD spectropolarimetry

CD spectra were acquired on a JASCO J-810 spectropolarimeter-fluorometer calibrated with (+)-10-camphorsulfonic acid and purged with N_2 at 20 liters/min (40). CD spectra of 1.5 μM or 5 μM His_6-porin samples were measured in the far-UV region (195–250 nm) as described previously (26). After correction by baseline subtraction, CD spectra were converted to mean residue ellipticity according to the formula:

$$[\theta]_M = M\theta/\{(10)(l)(c)(n)\},$$

where $[\theta]_M$ is deg cm^2 dmol^{-1} × 10^{-3}, M is the molecular weight of His_6-porin (31,402 g/mol), θ is the measured ellipticity in millidegrees, l is the path length of the cuvette in centimeters (0.1 cm for protein in detergent and 0.05 cm for protein in liposomes), c is the protein concentration in g/liter, and n is the number of amino acid residues in the protein (295). Twelve spectra were collected and averaged for each proteoliposome preparation; three spectra were collected and averaged for the protein in detergent. Far-UV spectra were deconvoluted with the CDSSTR algorithm (41–43) in the DichroWeb package (44).

Near-UV (245–330 nm) CD spectra of 33 μM His_6-porin in mixed detergents were measured with a JASCO J-810 spectropolarimeter-fluorometer, as described (26). Molar ellipticity was calculated from the baseline corrected spectra according to the formula: $[\theta] = M\theta/\{(10)(l)(c)\}$ where $[\theta]$ is the molar ellipticity (degrees cm^2 dmol^{-1}), and l is 1 or 5 cm. Proteoliposomes analyzed by near-UV CD were prepared with the FT technique, using 5–10 μM His_6-porin in either 3.5 mM SDS or 3.5 mM SDS and 30 mM DDM. In some cases, following this analysis, liposome-swelling assays of these samples were performed after dilution of the samples to 0.66 mg/ml phospholipid.

Temperature was controlled during thermal denaturation experiments using the Peltier device in the spectropolarimeter. Experiments were carried out with a ramp speed of 1°C/min; θ (mdeg) was monitored at 208 nm and at 268 nm at 1°C intervals, and full spectra were collected at 5°C intervals. The cuvettes used for these experiments had pathlengths of 0.1 cm (far-UV) and 1 cm (near-UV). HT voltage (absorbance) measurements were monitored during collection of CD data.

RESULTS

Reconstitution of His_6-porin into liposomes

Before the analysis of detergent-solubilized porin, it was necessary to characterize the conformation of mitochondrial porin embedded in a membrane. Such analyses cannot easily be performed in mitochondria because of the abundance of other proteins in the outer membrane. Therefore, His_6-porin was functionally reconstituted into liposomes and analyzed by far- and near-UV CD, and UV absorption spectroscopy, to provide a basis for comparison with detergent-solubilized protein.

His_6-porin solubilized in SDS or 3.5 mM SDS/30 mM DDM ($SDS_{3.5}DDM_{30}$, see below) could be integrated into liposomes using a FT procedure to generate osmotically responsive proteoliposomes (Fig. 2). As described by Colombini (35), the FT proteoliposomes were permeable to PEG of average molecular weight of 1000 but showed very little swelling in response to PEG 3350, supporting the conclusion that channels of wild-type dimensions were formed. The FT procedure was necessary for incorporation under the conditions used in this study. For both SDS-His_6-porin (data not shown) and $SDS_{3.5}DDM_{30}$-His_6-porin (Fig. 2 *B*) in FT liposomes, channel activity in response to sucrose was resistant to heating to 65°C, and a partial swelling response was seen after heating to 100°C.

Protease resistance is often used as a criterion for refolding of porins, such as human mitochondrial porin (hVDAC1) (45), and bacterial OmpA (27,46), after reconstitution into artificial membranes. It is also used to confirm that *Neurospora* mitochondrial porin is assembled in the outer membrane after in vitro import into isolated organelles (47). Therefore, the protease sensitivities of SDS- and $SDS_{3.5}DDM_{30}$-solubilized His_6-porin before and after reconstitution into liposomes were examined (Fig. 3). The sensitivity of porin obtained by dissolving isolated mitochondria in detergents was also tested. Immunoblotting was used to detect the low amounts of His_6-porin ($<2\ \mu M$) in liposomes and native porin in mitochondria. Trypsin was also detected on the immunoblots as 24- or 25-kDa bands as a result of sequence similarity between trypsin and the porin peptide (residues 7–20) used to generate antibodies used for this study.

Native porin is very susceptible to protease digestion after solubilization of mitochondria in 3.5 mM SDS (Fig. 3 *A*). In contrast, when the organelles are solubilized in $SDS_{3.5}DDM_{30}$, porin is highly resistant to digestion with trypsin. A minor 50-kDa species can also be observed after digestion of mitochondria in $SDS_{3.5}DDM_{30}$, suggestive of a porin dimer.

His_6-porin migrates with an apparent molecular mass of 32 kDa (Fig. 3 *B*). Digestion of $SDS_{3.5}DDM_{30}$-His_6-porin with trypsin resulted in a reduction but not complete elimination of the porin; species of ~20-kDa remained. His_6-porin in 3.5 mM SDS was digested, leaving some residual material of ~20 kDa. Undigested FT SDS and SDS/DDM-His_6-porin liposomes contained additional faint species of ~60 kDa and >100 kDa (Fig. 3 *C*), suggesting that dimers and multimers of the protein are present in the liposomes. After digestion with trypsin, the full-length His_6-porin band remained, but at less than half the intensity of the intact band in the undigested sample, and the higher molecular weight species was no longer detectable.

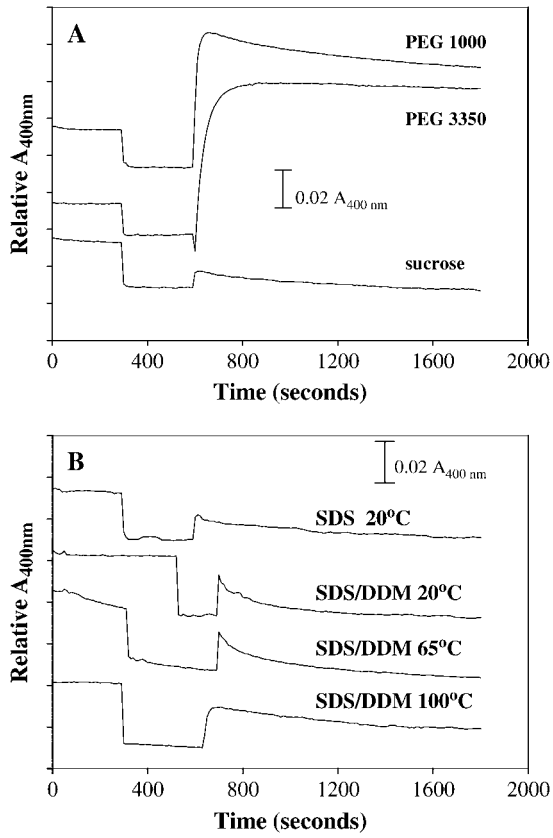

FIGURE 2 Liposome swelling assays. Proteoliposomes were prepared using $SDS_{3.5}$- and $SDS_{3.5}/DDM_{30}$-solubilized His_6-porin and the FT method. (*A*) Swelling in response to solutes of varying molecular weights. Swelling was measured by following absorbance at 400 nm after the addition of sucrose, PEG 1000, or PEG 3350, as indicated next to the trace. (*B*) Thermal stability of swelling in response to sucrose. Swelling was measured either directly (20°C) or after heating to 65°C or 100°C as indicated above each plot. In both panels, relative A_{400} values for each sample were plotted on the same scale, which permitted individual plots to be distinguishable from each other.

The combination of liposome swelling and protease resistance indicates that His_6-porin is embedded in proteoliposomes in a functional form. Far-UV CD analysis revealed a broad spectrum (Fig. 4 *A*); deconvolution confirmed high β-strand content (31%, Table 1), as expected for folded mitochondrial porin (for example, 31–38% for hVDAC1 in lipid bilayers, 45). The α-helical content of this form was very low (7%), similar to that seen for hVDAC1 (8–12%) (45). Increased temperature did not alter the overall shape of the far-UV spectra (Fig. 4 *A*).

The membrane-embedded state was further examined to provide reference data for comparisons with detergent-solubilized porin. The wavelength of maximum Trp fluorescence (λ_{max}Trp) is influenced by exposure of Trp residues

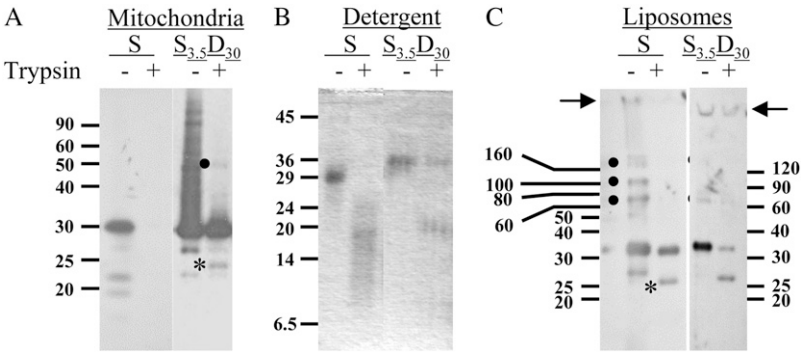

FIGURE 3 Protease susceptibility of porin in mitochondria, liposomes, and detergent. (*A*) Western blot analysis of *N. crassa* mitochondria. Mitochondria (2.5 μg protein/well) were solubilized in $SDS_{3.5}$ (S, lanes *1* and *2*) or $SDS_{3.5}DDM_{30}$ ($S_{3.5}D_{30}$, lanes *3* and *4*) and analyzed after a 30-min digestion in the absence (−) or presence (+) of 0.75 μg trypsin as indicated. Minor proteolytic fragments (~20 kDa) resulted from activity of mitochondrially associated proteases during isolation and/or the 30-min incubation at room temperature. Similar analysis was performed on (*B*) 7.5 μg of His_6-porin solubilized in 3.5 mM SDS (lanes *1* and *2*) or $SDS_{3.5}DDM_{30}$ (lanes *3* and *4*) and (*C*) FT proteoliposomes formed in the presence of 0.9 mM SDS/7 mM DDM and containing 2.5 μg His_6-porin. Samples were undigested (lanes *1* and *3*) or digested with 0.75 μg trypsin (lanes *2* and *4*). Panel *B* shows an image of the Coomassie blue-stained gel. The molecular weights of markers in the molecular weight ladder are indicated to the side of each panel. Solid circles indicated multimers of His_6-porin, and cross-reacting trypsin is indicated by asterisks. The trypsin band is not visible in lane 2 of panel *A* because of the short exposure used; it is visible in longer exposures (data not shown).

to solvent. λ_{max}Trp ranges from 347 to 351 nm for residues completely exposed to the solvent, to 308 nm for those in a highly hydrophobic environment without any possibility for hydrogen bonding (48,49). In liposomes, λ_{max}Trp of His_6-porin was 329 nm, similar to that observed for membrane-embedded hVDAC1 (45) and other β-barrel proteins (OEP, 16 (50); OmpA (51); FomA (52)).

Finally, near-UV spectropolarimetry was used to examine the tertiary interactions in the liposome-embedded protein. The near-UV spectrum of His_6-porin in proteoliposomes displayed positive ellipticity (Fig. 5 *A*), as does that of folded PorB class 2 (53) and class 3 (54) porins of *Neisseria*. Together, these spectroscopic features, combined with protease resistance, form the criteria for correctly folded His_6-porin in detergent systems.

Far-UV CD spectropolarimetry of His_6-porin in mixed detergent systems

Addition of a nonionic detergent to SDS-solubilized bacterial OmpA protein was shown to convert the α-helix-rich structure to one predominantly β-strand (29). Several detergent systems were examined to determine whether a similar approach would yield well-folded mitochondrial porin. SDS and DPC were chosen initially to solubilize His_6-porin, based on the high solubility of the protein in these detergents (26). Under these conditions, β-strand content is low and ranges from 18% to 25% (Table 1). The nonionic detergents, DDM and OG, and the zwitterionic LDAO were used as the second detergents in the system. Phase separation occurred at several LDAO/SDS ratios, limiting the mixtures that could be tested. For simplicity, mixtures will be described for each detergent, with its concentration in mM, as a subscript. For example, $SDS_{3.5}DDM_{7.5}$ is a mixture of 3.5 mM SDS and 7.5 mM DDM.

To determine the effects of secondary detergent addition on the protein solubilized in DPC or SDS, far-UV CD was used (Fig. 4 *B*, Table 1). In 3.5 mM SDS, and in $SDS_{3.5}DDM_{7.5}$, the far-UV spectrum of His_6-porin is typical of an α-helix-rich protein with a minimum at 208 nm and a shoulder at 220 nm. In $SDS_{3.5}DDM_{15}$, the spectrum of the protein exhibits a broad minimum in the 210- to 220-nm range, more typical of a β-strand-rich protein; deconvolution reveals a

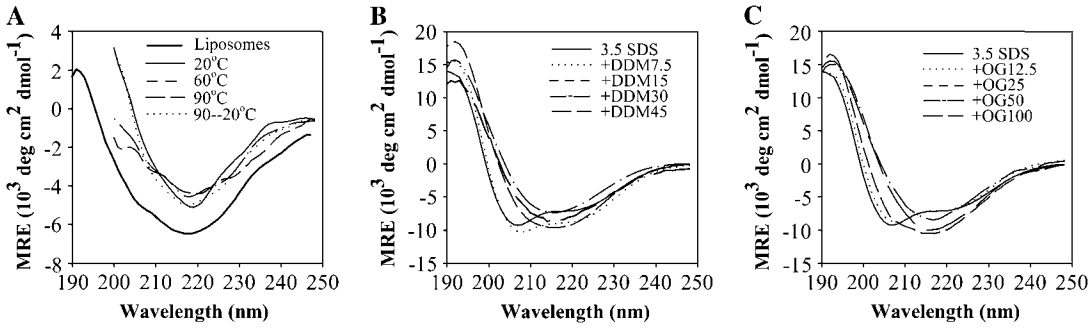

FIGURE 4 Far-UV CD analysis of 5 μM His_6-porin in (*A*) liposomes, (*B*) SDS/DDM systems, and (*C*) SDS/OG systems. Spectra were obtained as indicated in Materials and Methods. (*A*) Full-length spectrum of His_6-porin in liposomes (*thick line*). Thermal denaturation of porin in liposomes was followed, and far-UV spectra were obtained at 20°C (*solid line*), 60°C (*short dashed line*), and 90°C (*long dashed line*) and after cooling back to 20°C (*dotted line*). The cell used for thermal denaturation experiments did not allow collection of CD data below 200 nm. In panels *B* and *C*, detergent concentrations are indicated in legend; ''+DDM'' indicates the concentration (mM) of DDM that was added to 3.5 mM SDS.

TABLE 1 Analysis of His_6-porin solubilized in mixed detergent systems and proteoliposomes

Porin in	Detergent added	Temperature (°C)	α-Helix (%)	β-Strand (%)	Turn and unordered	Maximum concentration of soluble porin (μM)
3.5 mM SDS		20	32	18	50	66
	7.5 mM DDM	20	33	17	50	5*
	15 mM DDM	20	23	28	49	5*
	30 mM DDM	20	18	35	47	5*
	30 mM DDM	35	14	36	50	5*
	30 mM DDM	45	14	33	52	5*
	30 mM DDM	55	15	28	56	nd†
	30 mM DDM	60	12	28	60	nd
	30 mM DDM	80	14	31	55	nd
	30 mM DDM	95	ndc‡	ndc	ndc	nd
	30 mM DDM	95–20	13	29	57	nd
	45 mM DDM	20	13	38	49	5*
	12.5 mM OG	20	21	29	50	1.5
	25 mM OG	20	24	28	48	1.5
	50 mM OG	20	17	35	47	1.5
	100 mM OG	20	17	35	48	1.5
	40 mM LDAO	20	13	34	53	1.5
20 mM DPC		20	22	25	53	10
	7.5 mM DDM	20	14	33	54	1.5
	15 mM DDM	20	9	36	54	1.5
	30 mM DDM	20	9	38	53	1.5
	6.25 mM OG	20	13	29	58	1.5
	50 mM OG	20	7	35	57	1.5
	100 mM OG	20	6	38	56	1.5
	50 mM LDAO	20	16	33	51	5*
Liposomes		20	4	31	64	10

Far-UV spectropolarimetry was performed on either 1.5 or 5 μM porin samples as indicated; the resulting spectra were deconvoluted with CDSSTR.
*Higher concentrations not tested.
†Not determined because of protein precipitation in the sample.
‡Not deconvoluted because of poor spectrum at <200 nm.

loss of α-helix concomitant with an increase in β-strand to 28%. In $SDS_{3.5}DDM_{30}$ and $SDS_{3.5}DDM_{45}$, β-strand content reached 35% and 38%, respectively (Table 1). λ_{min} was 215–216 nm in $SDS_{3.5}DDM_{30}$, and $SDS_{3.5}DDM_{45}$. In liposomes, λ_{min} was 219–221 nm (Fig. 4). Similarly, λ_{min} of the β-barrel protein Tom40 (55) was red-shifted in liposomes compared to in detergent. The α-helical content of His_6-porin was higher in SDS/DDM (13–18%) than in liposomes (7%); a similar observation was made by Shanmugavadivu et al. (45) for human VDAC (14–18% in LDAO versus 8–12% in liposomes).

Addition of OG (Fig. 4 *C*) or LDAO (data not shown) to SDS-solubilized porin led to similar increases in β-strand structure (Table 1). Similarly, β-strand content increased on addition of DDM, OG, and LDAO to DPC-solubilized porin. However, these mixtures were found to be unsuitable for further structural studies because of the low porin solubility (~1.5 μM, Table 1) and phase separation that occurred in most DPC/LDAO mixtures.

SDS-solubilized His_6-porin is very stable during heating, and the limited unfolding that does occur is completely

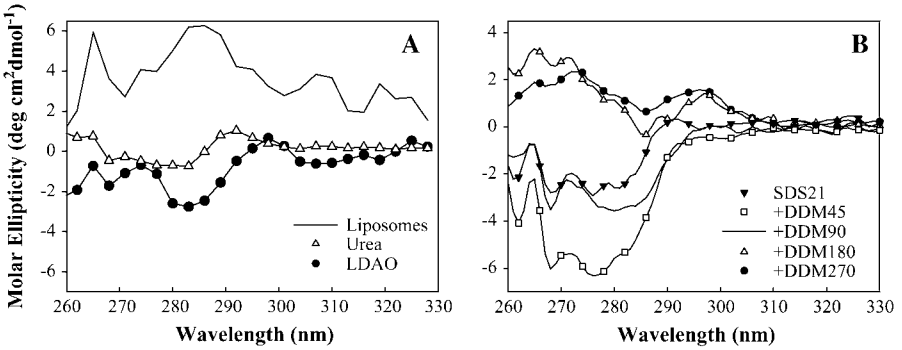

FIGURE 5 Near-UV analysis of 33 μM His_6-porin in mixed detergent systems. Spectra were obtained as described in Materials and Methods: (*A*) 8 M urea, 300 mM LDAO, and proteoliposomes; (*B*) SDS/DDM mixtures, as indicated. Detergent mixtures are identified as described for Fig. 4.

reversible (Fig. 6 *A*, Table 1). During heating of $SDS_{3.5}DDM_{30}$-solubilized porin to 45°C, there are only minor alterations to the secondary structural content (data not shown). At 55°C, an increase in the HT voltage, as monitored by the CD spectropolarimeter, indicated precipitation in the sample; absorbance measurements at the end of the experiment demonstrated that ~2/3 of the protein remained in solution. At 55°C and above, a conformational shift occurred, and the fraction of β-strand was reduced to ~28%, and random structure increased to 60% (Fig. 6 *B*). In contrast, thermal denaturation is not reversible in $SDS_{3.5}DDM_{30}$ (Fig. 6 *B*), and the secondary structure on cooling to 20°C remains similar to that measured at 55°C and above (Table 1).

Tryptophan fluorescence in mixed-detergent systems

The fluorescence of both His_6-porin and model compounds (Table 2) was used to determine how the addition of a second detergent to SDS or DPC micelles affects the interactions of tyrosine and tryptophan with the micelles. Two variants of each compound were used, the relatively hydrophobic O-alkyl-esters, BOC-Y-OMe and N-Ac-W-OEth, and the more hydrophilic amide variants, N-Ac-Y-NH_2 and N-Ac-W-NH_2. In previous studies, it was shown that the former compounds are better probes of the hydrophobic interiors of detergent micelles (26), whereas the latter sample both the surface and interior of the micelle.

In 3.5 mM SDS, both Trp model compounds are predominantly in the aqueous phase, although N-Ac-W-OEth interacts slightly more often with the micelle, as indicated by the slightly blue-shifted λ_{max}Trp (351 vs. 347 nm), compared with that of N-Ac-W-NH_2. Unlike that observed in aqueous buffer, fluorescence is quenched by SDS (26). In the SDS/DDM micelles, λ_{max}Trp of both Trp compounds is blue-shifted to near 340 nm, and the environment is less quenching (Table 2). In contrast, λ_{max}Trp was similar for both Trp compounds in DPC and DPC/DDM and DPC/OG mixtures. DPC/OG and DPC/DDM micelles quenched N-Ac-W-NH_2 fluorescence, but only the former reduced the fluorescence of N-Ac-W-OEth (Table 2). Thus, blue-shifts in fluorescence are seen only in the SDS background.

In 3.5 mM SDS, λ_{max}Trp for His_6-porin fluorescence is 336 nm, indicating that the Trp residues reside in a hydrophobic environment but are partially solvent exposed. The low intensity of the Trp fluorescence suggests strong quenching by the SDS headgroups (26). In the presence of increasing DDM concentrations, λ_{max}Trp is blue-shifted significantly, and the fluorescence intensity increases, indicating that, overall, the Trp residues are moving to a more hydrophobic, less quenching environment in the mixed micelles. Similar trends were observed in the SDS/OG system (Table 2), but a higher mole fraction of OG was required to induce the conformational shift. Blue-shifted Trp fluorescence was observed for His_6-porin in $DPC_{20}DDM_{30}$, but not in DPC/OG mixtures.

Tyrosine exposure in detergent-solubilized His_6-porin

Because of the large blue shifts in His_6-porin Trp fluorescence in the SDS/DDM mixtures, the overlap between the Tyr fluorescence and the blue-shifted Trp fluorescence is extensive, making it difficult to analyze (data not shown). Therefore, UV absorption spectroscopy was used to determine the exposure of Tyr to the aqueous environment. The second derivative plots of UV absorbance spectra (SDUV) were used to calculate *r* values; in general, higher *r* values indicate exposure to solvent, whereas lower values are indicative of interactions with hydrophobic environments (39). In SDS, *r* calculated for the more hydrophobic Tyr compound, BOC-Y-OMe, is lower (1.51) than that of the more hydrophilic compound N-Ac-Y-NH_2 (2.24). In $SDS_{3.5}DDM_{7.5}$ micelles, *r* values increase for both model compounds and then decrease in the presence of higher concentrations of DDM. For the more hydrophobic compound, *r* continues to decrease, suggesting increased interactions with the interior of the micelle. In contrast, in $SDS_{3.5}DDM_{30}$ micelles, exposure of the hydrophilic compound returns to near that observed in SDS alone.

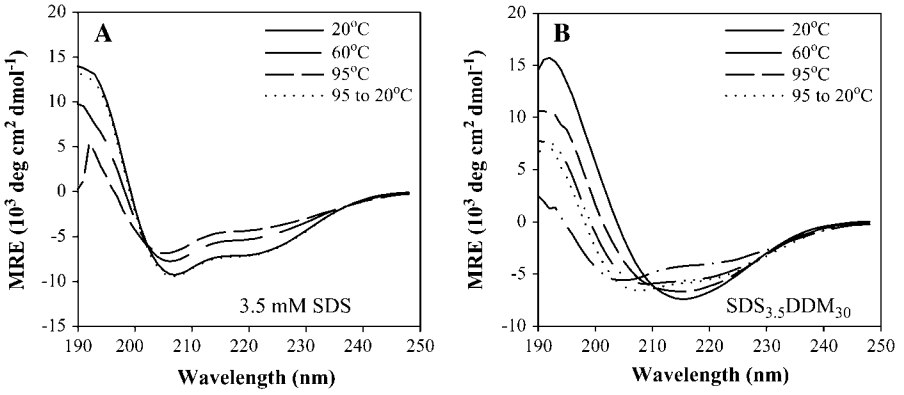

FIGURE 6 Thermal denaturation of His_6-porin as followed by far-UV CD spectropolarimetry. The experiments were carried out as described in Materials and Methods for His_6-porin in (*A*) 3.5 mM SDS and (*B*) $SDS_{3.5}DDM_{30}$. Temperatures at which the spectra were obtained are indicated on the graphs. Note that in *A*, the spectrum obtained after cooling from 95°C to 20°C is partially obscured by that at 20°C.

TABLE 2 Summary of fluorescence data collected at excitation wavelengths of 280 nm (Tyr) and 296 (Trp) nm

	His_6-porin		N-Ac-W-OEth		N-Ac-W-NH_2	
	Trp		Trp		Trp	
	λ_{max}	Int_{max}*	λ_{max}	Int_{max}	λ_{max}	Int_{max}
Sample in 3.5 mM SDS with						
No addition	336	0.03	347	0.04	351	0.11
7.5 mM DDM	337	0.03	341	0.07	348	0.12
15 mM DDM	330	0.11	337	0.13	345	0.13
30 mM DDM	322	0.08	343	0.08	340	0.17
12.5 mM OG	339	0.05	347	0.09	349	0.15
25 mM OG	333	0.09	347	0.07	350	0.12
50 mM OG	330	0.08	345	0.10	352	0.13
100 mM OG	330	0.07	342	0.07	347	0.16
Sample in 20 mM DPC with						
No addition	337	0.06	337	0.22	342	0.25
7.5 mM DDM	335	0.05	337	0.21	343	0.09
30 mM DDM	327	0.17	338	0.22	338	0.09
12.5 mM OG	333	0.09	338	0.11	342	0.11
50 mM OG	334	0.07	339	0.11	342	0.12
100 mM OG	334	0.07	338	0.09	342	0.11

His_6-porin and amino model compounds were solubilized in the detergent mixtures indicated. Maximum intensity (Int_{max}) values were corrected for differences in concentration.
*Intensity of fluorescence at λ_{max}, corrected for protein concentration.

Tyr exposure is high ($r = 1.39$, $Y_{exp} = 77\%$) in SDS-solubilized porin (Table 3). However, on average, only 22% (~2) of the 9 Tyr residues in the presence of $SDS_{3.5}DDM_{7.5}$ are exposed to the aqueous environment ($r = 0.85$, Table 3). This observation confirms the prediction that increased Tyr fluorescence intensity in the SDS/DDM system reflects a higher degree of interaction between the Tyr residues and the detergent micelles. At higher DDM concentrations (15–30 mM) in SDS, Tyr exposure is near 50%, suggesting a further change in conformation when the concentration of DDM exceeds 15 mM.

Near-UV CD spectropolarimetry

To investigate whether alterations in tertiary interactions accompany the structural changes detected by the methods described above, near-UV CD spectropolarimetry was used (Fig. 5 *B*). Higher concentrations of detergent were required to solubilize sufficient amounts of protein for these studies, but the same molar ratios of the pairs of surfactants were used. The protein was first solubilized in 21 mM SDS, followed by addition of DDM to final concentrations ranging from 45 to 270 mM. In SDS alone, near-UV CD spectra of porin display strong negative ellipticity in the 260- to 290-nm range, which includes signals from Trp (270–290 nm) and Tyr (265–270 nm). Higher negative ellipticities in the Tyr and the Trp regions of the spectra are observed in $SDS_{21}DDM_{45}$ (Fig. 5 *B*). In $SDS_{21}DDM_{90}$, the overall shape of the spectrum is similar to that of the protein in urea or LDAO (Fig. 5 *A*) (26), but the negative intensity is intermediate between that in urea and that in $SDS_{21}DDM_{45}$. Remarkably, the ellipticity is positive in $SDS_{21}DDM_{180}$ and $SDS_{21}DDM_{270}$, as shown for porin in liposomes (Fig. 5 *A*).

To assess the stability of the tertiary interactions, thermal denaturation was followed by near-UV CD. In SDS, the secondary structure composition of porin is not altered

TABLE 3 Second derivative plots of UV absorbance spectra analysis of His_6-porin and model compounds

	r			
Detergents	N-Ac-W-OEth + BOC-Y-OMe	N-Ac-W-NH_2 + N-Ac-Y-NH_2	His_6-porin	Y_{exp} (α)
3.5 mM SDS	1.51	2.24	1.39	0.77
7.5 mM DDM + 3.5 mM SDS	1.82	2.48	0.85	0.22
15 mM DDM + 3.5 mM SDS	1.53	1.63	1.02	0.42
20 mM DDM + 3.5 mM SDS	1.59	1.80	1.16	0.55
30 mM DDM + 3.5 mM SDS	0.85	2.26	1.18	0.58

r and Y_{exp} values were calculated as described in Materials and Methods. For the amide model compounds and His_6-porin, each experiment was repeated at least twice; averages are reported; standard deviations were <22%. For the hydrophobic compounds, the data reported are from a single experiment.

significantly by heating to 95°C (Fig. 6). However, heating alters the near-UV CD spectrum (Fig. 7 *A*); above 40°C, the spectra show very little ellipticity. The spectrum obtained after cooling of the heated sample to 20°C is similar in shape to that of the unheated sample, but the signal intensity has increased.

During heating, the near-UV CD spectra of the protein in $SDS_{21}DDM_{180}$ show a steady decrease in ellipticity until 40°C is reached (Fig. 7 *B*). At this point the spectrum resembles the partially unfolded state of the protein seen in 8 M urea; at higher temperatures, the spectra display negative ellipticity (Fig. 5 *A*). Protein precipitation is occurring at this temperature, as detected by an increase in HT voltage (data not shown). Absorbance measurements taken after the completion of the experiment indicate that ~⅓ of the protein remained in solution. Thermal denaturation is nonreversible, as the near-UV spectra obtained after cooling of the sample to 20°C is very similar to that seen at 90°C (Fig. 7 *A*).

DISCUSSION

The results presented here indicate that an SDS/DDM mixture maintains high concentrations of His_6-porin in a β-strand-rich state with tertiary contacts that resembles the membrane-embedded pore. In terms of Tyr fluorescence, β-strand content, and protease resistance, both the liposome-embedded and SDS/DDM-solubilized forms resemble membrane-embedded hVDAC1 (45). NMR spectroscopy was recently used to analyze LDAO-solubilized hVDAC1. In this case the criteria for folding were perturbations in the NMR spectrum after incubation of the protein with ATP or β-NADH (9). These compounds are known to influence pore conductivity in black lipid bilayers (4,6,56). In contrast, extensive tertiary contacts were not detected by near-UV CD in *N. crassa* mitochondrial porin folded in LDAO after acetone precipitation (26), suggesting that the procedure for refolding is critical.

Additions of different molar ratios of DDM and SDS to porin promoted unique conformations, which are summarized in Fig. 8. In $SDS_{3.5}DDM_{7.5}$ mixtures, the overall secondary structure content and λ_{max}Trp are similar to those in SDS alone. However, rearrangements involving Tyr residues occur, as indicated by the large decrease in Tyr exposure and increased negative ellipticity in the Tyr region of the near-UV CD spectrum (Fig. 5 *B*). Because the α-helix and β-strand content are unchanged from those in SDS alone, these rearrangements are likely occurring within the turns or unordered regions of the protein in SDS. Seven of the nine Tyr are clustered in the C-terminal half of the protein (Fig. 1), suggesting that this segment is unordered in the SDS-solubilized protein.

In $SDS_{3.5}DDM_{15}$, there is a notable increase in β-strand at the expense of α-helical structure. This rearrangement involves placement of Trp residues in hydrophobic environments, as evidenced by the blue-shift of λ_{max}Trp. To date, all models of mitochondrial porin structure (20,57,58) place the two Trp residues near or in predicted transmembrane β-strands (Fig. 1, for example). It is tempting to speculate that the regions of the protein flanking the two Trp residues are in α-helices in SDS and are rearranged into β-strands in $SDS_{3.5}DDM_{15}$. Near-UV CD analysis suggests that the tertiary interactions involving Trp are less extensive in this conformation. Accompanying the change in secondary structure, Tyr exposure and negative ellipticity in the Tyr region of the near-UV CD spectrum are further reduced, suggesting significant changes to the folded state of large segments of the protein.

Higher DDM concentrations ($SDS_{3.5}DDM_{30}$) promote a higher level of β-strand (35%) with a concomitant decrease in α-helix. A large blue shift in λ_{max}Trp is observed, indicating that the Trp residues are hydrogen-bonded in a very hydrophobic environment, as predicted in numerous structural models for *Neurospora* mitochondrial porin (1,57–59) (see Fig. 1). On average, half of the Tyr residues are solvent exposed at the elevated DDM concentrations that yield high β-sheet content and suggest formation of a folded β-barrel. About half of the tyrosines are predicted to be solvent-exposed in the folded protein in several models (57,58), whereas in other models all or almost all of the tyrosines reside outside of predicted transmembrane regions (1,59).

The near-UV CD spectrum of His_6-porin in SDS_{21}/DDM_{270} displays positive ellipticity in both the Tyr and Trp regions. Because there are no near-UV data for natively folded mitochondrial porins, comparisons can only be made

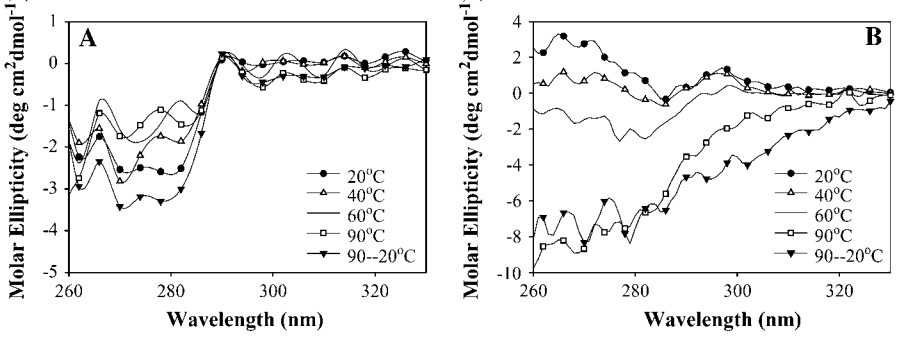

FIGURE 7 Thermal denaturation of His_6-porin in (*A*) 21 mM SDS and (*B*) $SDS_{3.5}DDM_{180}$, as measured by near-UV CD spectropolarimetry. Experiments were carried out as described in Materials and Methods. Temperatures at which the spectra were taken are indicated in the panels.

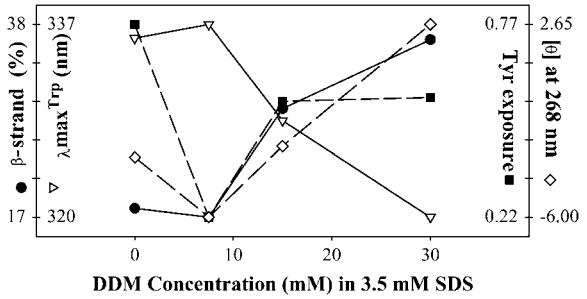

FIGURE 8 Summary of the folded state of His_6-porin in SDS/DDM systems. Composite figure showing the differences in β-strand content (*solid circles*), λ_{max}Trp (*open triangles*), Tyr exposure (*solid squares*), and molar ellipticity at 268 nm (*open diamonds*). All values were adjusted to the same arbitrary scale; the exact values of each parameter are listed on the *x* axis in the same column as the descriptor for that parameter.

with bacterial proteins. Positive ellipticity has been reported in the near-UV CD spectra of the folded forms of the PorB class 2 (53) and class 3 (54) porins of *Neisseria* and for the β-barrel segment of OmpA (29). As observed for mitochondrial porin, the CD spectrum of OmpA in SDS is negative, but on folding by the addition of OG, it is dominated by a positive signal (29). Although the correlation is not absolute (60), a conversion from positive to negative ellipticity accompanies unfolding of water-soluble β-strand proteins, such as cardiotoxin analog III (CTXIII, (61,62)), CD40L (63), and TNF-α (64).

Recombinant His_6-porin was incorporated into liposomes, resulting in osmotically responsive proteoliposomes that were useful for comparison to detergent-solubilized mitochondrial porins. His_6-porin in both SDS and SDS/DDM could be incorporated into proteoliposomes by a FT procedure, but neither could insert directly after dilution into preformed liposomes. In contrast, OmpA (34) and human VDAC1 (45) spontaneously insert into membranes when diluted into a solution of liposomes. The difference may in part be explained by the fact that the latter system utilized 1,2-diacyl-*sn*-glycerol-3-phosphocholine lipids at pH 3 in citrate buffer, whereas the system described in this work utilized a mixture of L-α-phosphatidyl choline and L-α-phosphatidic acid at pH 7 (11).

It is noteworthy that porin oligomers were detected in both liposomes and SDS/DDM-solubilized mitochondria (Fig. 2) but not in mitochondria in the absence of detergent. Although the urea included in the SDS-PAGE gels presented in this study might disrupt such interactions, oligomers were also undetectable in mitochondria analyzed with gels lacking denaturant (data not shown). Furthermore, they were not detected in two-dimensional arrays of mitochondrial outer membranes from *N. crassa* (15–17). In contrast, chemical cross-linking allowed detection of the oligomers of rat liver (65) and hVDAC1 (9). Although mitochondrial porin may be able to oligomerize under certain conditions, interactions with other proteins (9,66) and porin-associated sterols (67) may prevent the formation of oligomers in the mitochondrial outer membrane.

Taken together, these studies reveal that a mixture of SDS and DDM promotes a His_6-porin conformation very similar to that adopted by the protein functionally reconstituted into artificial membranes. The identification of a mixed detergent system for well-folded mitochondrial porin is an important first step toward high-resolution structural studies using approaches such as NMR spectroscopy, which has recently been used to analyze hVDAC1 (9) and OmpA and OmpX solubilized in detergent (68–71).

We thank Lydia Chen, Anh Tran, and William Summers for excellent technical assistance, Jamie Galka and Darren Manley for valuable discussions, and Matt Young for his continued encouragement and support. The comments of the reviewers of this manuscript are also greatly appreciated.

This work was supported by Discovery Grants from the Natural Sciences and Engineering Research Council to D.A.C. and J.D.O., funds from the University of Manitoba Research Grants Program (D.A.C.), and a Manitoba Health Research Council Graduate Fellowship to D.C.B.

REFERENCES

1. Benz, R. 1994. Permeation of hydrophilic solutes through mitochondrial outer membranes: review on mitochondrial porins. *Biochim. Biophys. Acta.* 1197:167–196.
2. Arora, K. K., C. R. Filburn, and P. L. Pedersen. 1993. Structure/function relationships in hexokinase. Site-directed mutational analyses and characterization of overexpressed fragments implicate different functions for the N- and C-terminal halves of the enzyme. *J. Biol. Chem.* 268:18259–18266.
3. Brdiczka, D., P. Kaldis, and T. Wallimann. 1994. In vitro complex formation between the octamer of mitochondrial creatine kinase and porin. *J. Biol. Chem.* 269:27640–27644.
4. Rostovtseva, T., and M. Colombini. 1996. ATP flux is controlled by a voltage-gated channel from the mitochondrial outer membrane. *J. Biol. Chem.* 271:28006–28008.
5. Rostovtseva, T., and M. Colombini. 1997. VDAC channels mediate and gate the flow of ATP: implications for the regulation of mitochondrial function. *Biophys. J.* 72:1954–1962.
6. Zizi, M., M. Forte, E. Blachly-Dyson, and M. Colombini. 1994. NADH regulates the gating of VDAC, the mitochondrial outer membrane channel. *J. Biol. Chem.* 269:1614–1616.
7. Crompton, M., S. Virji, V. Doyle, N. Johnson, and J. M. Ward. 1999. The mitochondrial permeability transition pore. *Biochem. Soc. Symp.* 66:167–179.
8. Shoshan-Barmatz, V., A. Israelson, D. Brdiczka, and S. S. Sheu. 2006. The voltage-dependent anion channel (VDAC): function in intracellular signalling, cell life and cell death. *Curr. Pharm. Des.* 12:2249–2270.
9. Malia, T. J., and G. Wagner. 2007. NMR structural investigation of the mitochondrial outer membrane protein VDAC and its interaction with antiapoptotic Bcl-xL. *Biochemistry.* 46:514–525.
10. Blachly-Dyson, E., and M. Forte. 2001. VDAC channels. *IUBMB Life.* 52:113–118.
11. Shao, L., K. W. Kinnally, and C. A. Mannella. 1996. Circular dichroism studies of the mitochondrial channel, VDAC, from *Neurospora crassa*. *Biophys. J.* 71:778–786.
12. Popp, B., S. Gebauer, K. Fischer, U. I. Flügge, and R. Benz. 1997. Study of structure and function of recombinant pea root plastid porin by biophysical methods. *Biochemistry.* 36:2844–2852.
13. Koppel, D. A., K. W. Kinnally, P. Masters, M. Forte, E. Blachly-Dyson, and C. A. Mannella. 1998. Bacterial expression and characterization of

the mitochondrial outer membrane channel. Effects of N-terminal modifications. *J. Biol. Chem.* 273:13794–13800.

14. Runke, G., E. Maier, J. D. O'Neil, R. Benz, and D. A. Court. 2000. Functional characterization of the conserved ''GLK'' motif in mitochondrial porin from *Neurospora crassa*. *J. Bioenerg. Biomembr.* 32: 563–570.
15. Mannella, C. A. 1989. Fusion of the mitochondrial outer membrane: use in forming large, two-dimensional crystals of the voltage-dependent, anion-selective channel protein. *Biochim. Biophys. Acta.* 981:15–20.
16. Thomas, L., E. Kocsis, M. Colombini, E. Erbe, B. L. Trus, and A. C. Steven. 1991. Surface topography and molecular stoichiometry of the mitochondrial channel, VDAC, in crystalline arrays. *J. Struct. Biol.* 106:161–171.
17. Guo, X. W., and C. A. Mannella. 1993. Conformational change in the mitochondrial channel, VDAC, detected by electron cryo-microscopy. *Biophys. J.* 64:545–549.
18. Dolder, M., K. Zeth, P. Tittmann, H. Gross, W. Welte, and T. Wallimann. 1999. Crystallization of the human, mitochondrial voltage-dependent anion-selective channel in the presence of phospholipids. *J. Struct. Biol.* 127:64–71.
19. Schulz, G. E. 2000. β-Barrel membrane proteins. *Curr. Opin. Struct. Biol.* 10:443–447.
20. Bay, D. C., and D. A. Court. 2002. Origami in the outer membrane: the transmembrane arrangement of mitochondrial porins. *Biochem. Cell Biol.* 80:551–562.
21. Colombini, M. 1980. Structure and mode of action of a voltage dependent anion-selective channel (VDAC) located in the outer mitochondrial membrane. *Ann. N. Y. Acad. Sci.* 341:552–563.
22. Roos, N., R. Benz, and D. Brdiczka. 1982. Identification and characterization of the pore-forming protein in the outer membrane of rat liver mitochondria. *Biochim. Biophys. Acta.* 686:204–214.
23. Freitag, H., G. Genchi, R. Benz, F. Palmieri, and W. Neupert. 1982. Isolation of mitochondrial porin from *Neurospora crassa*. *FEBS Lett.* 145:72–76.
24. Troll, H., D. Malchow, A. Muller-Taubenberger, B. Humbel, F. Lottspeich, M. Ecke, G. Gerisch, A. Schmid, and R. Benz. 1992. Purification, functional characterization, and cDNA sequencing of mitochondrial porin from *Dictyostelium discoideum*. *J. Biol. Chem.* 267:21072–21079.
25. Aljamal, J. A., G. Genchi, V. De Pinto, L. Stefanizzi, A. De Santis, R. Benz, and F. Palmieri. 1993. Purification and characterization of porin from corn (*Zea mays L.*) mitochondria. *Plant Physiol.* 102:615–621.
26. Bay, D. C. 2007. The spectroscopic characterization of mitochondrial porin in membrane mimetic systems. PhD thesis. University of Manitoba, Winnipeg, Manitoba, Canada.
27. Dornmair, K., H. Kiefer, and F. Jahnig. 1990. Refolding of an integral membrane protein. OmpA of *Escherichia coli*. *J. Biol. Chem.* 265: 18907–18911.
28. Ohnishi, S., K. Kameyama, and T. Takagi. 1998. Characterization of a heat modifiable protein, Escherichia coli outer membrane protein OmpA in binary surfactant system of sodium dodecyl sulfate and octylglucoside. *Biochim. Biophys. Acta.* 1375:101–109.
29. Ohnishi, S., and K. Kameyama. 2001. *Escherichia coli* OmpA retains a folded structure in the presence of sodium dodecyl sulfate due to a high kinetic barrier to unfolding. *Biochim. Biophys. Acta.* 1515:159–166.
30. Otzen, D. E. 2003. Folding of DsbB in mixed micelles: a kinetic analysis of the stability of a bacterial membrane protein. *J. Mol. Biol.* 330:641–649.
31. Webb, D. C., and A. W. Cripps. 1999. A method for the purification and refolding of a recombinant form of the nontypeable *Haemophilus influenzae* P5 outer membrane protein fused to polyhistidine. *Protein Expr. Purif.* 15:1–7.
32. Lau, F. W., and J. U. Bowie. 1997. A method for assessing the stability of a membrane protein. *Biochemistry.* 36:5884–5892.
33. Popp, B., D. A. Court, R. Benz, W. Neupert, and R. Lill. 1996. The role of the N and C termini of recombinant *Neurospora* mitochondrial porin in channel formation and voltage-dependent gating. *J. Biol. Chem.* 271:13593–13599.
34. Surrey, T., and F. Jahnig. 1995. Kinetics of folding and membrane insertion of a beta-barrel membrane protein. *J. Biol. Chem.* 270:28199–28203.
35. Colombini, M. 1980. Pore size and properties of channels isolated from mitochondria isolated from *Neurospora crassa*. *J. Membr. Biol.* 53: 79–84.
36. Ninomiya, Y., K. Suzuki, C. Ishii, and H. Inoue. 2004. Highly efficient gene replacements in *Neurospora* strains deficient for nonhomologous end-joining. *Proc. Natl. Acad. Sci. USA.* 101:12248–12253.
37. Harkness, T. A., R. L. Metzenberg, H. Schneider, R. Lill, W. Neupert, and F. E. Nargang. 1994. Inactivation of the *Neurospora crassa* gene encoding the mitochondrial protein import receptor MOM19 by the technique of ''sheltered RIP''. *Genetics.* 136:107–118.
38. Laemmli, U. K. 1970. Cleavage of structural proteins during the assembly of the head of bacteriophage T4. *Nature.* 227:680–685.
39. Ragone, R., G. Colonna, C. Balestrieri, L. Servillo, and G. Irace. 1984. Determination of tyrosine exposure in proteins by second-derivative spectroscopy. *Biochemistry.* 23:1871–1875.
40. Manley, D., and J. D. O'Neil. 2003. Preparation of glycerol facilitator for protein structure and folding studies in solution. *Methods Mol. Biol.* 228:89–101.
41. Compton, L. A., and W. C. Johnson, Jr. 1986. Analysis of protein circular dichroism spectra for secondary structure using a simple matrix multiplication. *Anal. Biochem.* 155:155–167.
42. Manavalan, P., and W. C. Johnson, Jr. 1987. Variable selection method improves the prediction of protein secondary structure from circular dichroism spectra. *Anal. Biochem.* 167:76–85.
43. Sreerama, N., S. Y. Venyaminov, and R. W. Woody. 2000. Estimation of protein secondary structure from circular dichroism spectra: inclusion of denatured proteins with native proteins in the analysis. *Anal. Biochem.* 287:243–251.
44. Whitmore, L., and B. A. Wallace. 2004. DICHROWEB, an online server for protein secondary structure analyses from circular dichroism spectroscopic data. *Nucleic Acids Res.* 32:W668–W673.
45. Shanmugavadivu, B., H. J. Apell, T. Meins, K. Zeth, and J. H. Kleinschmidt. 2007. Correct folding of the beta-barrel of the human membrane protein VDAC requires a lipid bilayer. *J. Mol. Biol.* 368: 66–78.
46. Kleinschmidt, J. H., and L. K. Tamm. 1996. Folding intermediates of a beta-barrel membrane protein. Kinetic evidence for a multi-step membrane insertion mechanism. *Biochemistry.* 35:12993–13000.
47. Freitag, H., M. Janes, and W. Neupert. 1982. Biosynthesis of mitochondrial porin and insertion into the outer mitochondrial membrane of *Neurospora crassa*. *Eur. J. Biochem.* 126:197–202.
48. Burstein, E. A., N. S. Vedenkina, and M. N. Ivkova. 1973. Fluorescence and the location of tryptophan residues in protein molecules. *Photochem. Photobiol.* 18:263–279.
49. Reshetnyak, Y. K., Y. Koshevnik, and E. A. Burstein. 2001. Decomposition of protein tryptophan fluorescence spectra into log-normal components. III. Correlation between fluorescence and microenvironment parameters of individual tryptophan residues. *Biophys. J.* 81:1735–1758.
50. Linke, D., J. Frank, J. F. Holzwarth, J. Soll, C. Boettcher, and P. Fromme. 2000. In vitro reconstitution and biophysical characterization of OEP16, an outer envelope pore protein of pea chloroplasts. *Biochemistry.* 39:11050–11056.
51. Kleinschmidt, J. H., and L. K. Tamm. 2002. Secondary and tertiary structure formation of the beta-barrel membrane protein OmpA is synchronized and depends on membrane thickness. *J. Mol. Biol.* 324: 319–330.
52. Pocanschi, C. L., H. J. Apell, P. Puntervoll, B. Hogh, H. B. Jensen, W. Welte, and J. H. Kleinschmidt. 2006. The major outer membrane protein of *Fusobacterium nucleatum* (FomA) folds and inserts into lipid bilayers via parallel folding pathways. *J. Mol. Biol.* 355:548–561.

53. Minetti, C. A., J. Y. Tai, M. S. Blake, J. K. Pullen, S. M. Liang, and D. P. Remeta. 1997. Structural and functional characterization of a recombinant PorB class 2 protein from *Neisseria meningitidis*. Conformational stability and porin activity. *J. Biol. Chem.* 272:10710–10720.

54. Minetti, C. A., M. S. Blake, and D. P. Remeta. 1998. Characterization of the structure, function, and conformational stability of PorB class 3 protein from *Neisseria meningitidis*. A porin with unusual physicochemical properties. *J. Biol. Chem.* 273:25329–25338.

55. Becker, L., M. Bannwarth, C. Meisinger, K. Hill, K. Model, T. Krimmer, R. Casadio, K. N. Truscott, G. E. Schulz, N. Pfanner, and Wagner, R. 2005. Preprotein translocase of the outer mitochondrial membrane: reconstituted Tom40 forms a characteristic TOM pore. *J. Mol. Biol.* 353:1011–1020.

56. Runke, G., E. Maier, J. D. O'Neil, R. Benz, and D. A. Court. 2000. Functional characterization of the conserved ''GLK'' motif in mitochondrial porin from *Neurospora crassa*. *J. Bioenerg. Biomembr.* 32: 563–570.

57. Casadio, R., I. Jacoboni, A. Messina, and V. De Pinto. 2002. A 3D model of the voltage-dependent anion channel (VDAC). *FEBS Lett.* 520:1–7.

58. Runke, G., E. Maier, W. A. Summers, D. C. Bay, R. Benz, and D. A. Court. 2006. Deletion variants of *Neurospora* mitochondrial porin: electrophysiological and spectroscopic analysis. *Biophys. J.* 90:3155–3164.

59. Song, J., C. Midson, E. Blachly-Dyson, M. Forte, and M. Colombini. 1998. The topology of VDAC as probed by biotin modification. *J. Biol. Chem.* 273:24406–24413.

60. Bousquet, J. A., C. Garbay, B. P. Roques, and Y. Mely. 2000. Circular dichroic investigation of the native and non-native conformational states of the growth factor receptor-binding protein 2 N-terminal src homology domain 3: effect of binding to a proline-rich peptide from guanine nucleotide exchange factor. *Biochemistry.* 39:7722–7735.

61. Kumar, T. K., G. Jayaraman, C. S. Lee, T. Sivaraman, W. Y. Lin, and C. Yu. 1995. Identification of ''molten globule''-like state in all beta-sheet protein. *Biochem. Biophys. Res. Commun.* 207:536–543.

62. Sivaraman, T., T. K. Kumar, G. Jayaraman, C. C. Han, and C. Yu. 1997. Characterization of a partially structured state in an all-beta-sheet protein. *Biochem. J.* 321:457–464.

63. Matsuura, J. E., A. E. Morris, R. R. Ketchem, E. H. Braswell, R. Klinke, W. R. Gombotz, and R. L. Remmele, Jr. 2001. Biophysical characterization of a soluble CD40 ligand (CD154) coiled-coil trimer: evidence of a reversible acid-denatured molten globule. *Arch. Biochem. Biophys.* 392:208–218.

64. Narhi, L. O., J. S. Philo, T. Li, M. Zhang, B. Samal, and T. Arakawa. 1996. Induction of alpha-helix in the beta-sheet protein tumor necrosis factor-alpha: thermal- and trifluoroethanol-induced denaturation at neutral pH. *Biochemistry.* 35:11447–11453.

65. Zalk, R., A. Israelson, E. S. Garty, H. Azoulay-Zohar, and V. Shoshan-Barmatz. 2005. Oligomeric states of the voltage-dependent anion channel and cytochrome *c* release from mitochondria. *Biochem. J.* 386:73–83.

66. Roman, I., J. Figys, G. Steurs, and M. Zizi. 2006. Hunting interactomes of a membrane protein: obtaining the largest set of VDAC-interacting protein epitopes. *Mol. Cell. Proteomics.* 9:1667–1680.

67. De Pinto, V., R. Benz, and F. Palmieri. 1989. Interaction of non-classical detergents with the mitochondrial porin. A new purification procedure and characterization of the pore-forming unit. *Eur. J. Biochem.* 183:179–187.

68. Arora, A., F. Abildgaard, J. H. Bushweller, and L. K. Tamm. 2001. Structure of outer membrane protein A transmembrane domain by NMR spectroscopy. *Nat. Struct. Biol.* 8:334–338.

69. Fernández, C., C. Hilty, S. Bonjour, K. Adeishvili, K. Pervushin, and K. Wüthrich. 2001. Solution NMR studies of the integral membrane proteins OmpX and OmpA from *Escherichia coli*. *FEBS Lett.* 504:173–178.

70. Fernández, C., K. Adeishvili, and K. Wüthrich. 2001. Transverse relaxation-optimized NMR spectroscopy with the outer membrane protein OmpX in dihexanoyl phosphatidylcholine micelles. *Proc. Natl. Acad. Sci. USA.* 98:2358–2363.

71. Fernández, C., C. Hilty, G. Wider, P. Guntert, and K. Wüthrich. 2004. NMR structure of the integral membrane protein OmpX. *J. Mol. Biol.* 336:1211–1221.